Available online at www.sciencedirect.com

ScienceDirect

Procedia Engineering 2 (2010) 547–554

Procedia Engineering

www.elsevier.com/locate/procedia

Fatigue 2010

X-ray Computed Tomography vs. Metallography for Pore Sizing and Fatigue of Cast Al-alloys

Gianni Nicoletto[a]*, Giancarlo Anzelotti[a] and Radomila Konečná[b]

[a] *University of Parma, Dept. of Industrial Engineering, Parma, Italy.*
[b] *University of Žilina, Dept. of Materials Engineering, Žilina, Slovakia.*

Received 25 February 2010; revised 11 March 2010; accepted 15 March 2010

Abstract

Pores associated to the casting process are highly detrimental to the fatigue behavior of Al-Si alloys. The severity of casting pores in fatigue is related to a number of factors, such as pore size, morphology, position within the cast part, etc.. Metallography is readily applied to statistical pore characterization. However, random 2-D sections through pores do not provide good estimates of the defect size without further data analysis. In this contribution two experimental techniques, namely X-ray computed tomography and metallography, are applied to cast AlSi7Mg to characterize the size and morphology of casting pores. The 3D evidence provided by XCT is used to discuss pore sizing criteria based on metallographic measurements. The stress concentration due to the real 3D pore morphology is then investigated with finite element method and compared to simplified 2D pore models.

Keywords: cast AlSi alloy, porosity, X-ray CT, metallography, fatigue, finite element

1. Introduction

Cast Al-Si alloys are widely used in automotive applications due to increasing requirements to reduce weight, improve energy efficiency, and minimize environmental impact. Unfortunately, casting processes usually generate coarse microstructures and a variety of defects, namely pores and oxides, [1]. Porosity elimination of cast Al-Si parts is not realistic in the industrial context due to cost increments. Therefore, presence, severity and acceptability of porosity in cast parts should be verified and quantified during part and process development.

Porosity has been demonstrated to be highly detrimental to the fatigue behavior of cast aluminum-silicon alloys, [1-9]. Studies have indicated that a fatigue crack can rapidly initiate from large pores situated near or at the specimen surface, see Fig. 1a. As a result, the total fatigue life is dominated by the fatigue crack propagation phase, from the initiating pore to the final crack length as controlled by the material toughness. For a given initial crack (defect) size, the fatigue life of a material can be estimated within an order of magnitude, with a number of empirical models based on traditional linear elastic fracture mechanics, [7,9].

* Corresponding author. Tel.: +39-0521-905884 fax: +39-0521-905705
E-mail address: gianni.nicoletto@unipr.it.

1877-7058
doi:10.1016/j.proeng.2010.03.059

Assumption of the initial pore size for life prediction estimates should depend on the knowledge of the defect population. Statistical methods of pore sizing based on metallographic inspection have been proposed, [9, 10]. Typically, measurements of the equivalent size of the largest pore in numerous magnified fields of view are fitted to a statistical distribution that is used for extrapolating pore size expected in large, realistic material cross-sections.

The definition of the equivalent size of a casting pore is not straightforward as it is affected by the pore morphology, which depends on the formation process, [9]. Gas pores are typically spherical and therefore appear as rounded in a metallographic cross-section. On the other hand, microshrinkage pores are interdendritic cavities with branches that can appear with a variety and complexity of forms in a metallographic section. Fig. 1b shows a magnified view of a hypoeutectic Al-Si alloy with microshrinkage pores. While this cross-sectional view allows measurement of size and elongation of the individual pores, their actual shape in 3D remains unknown.

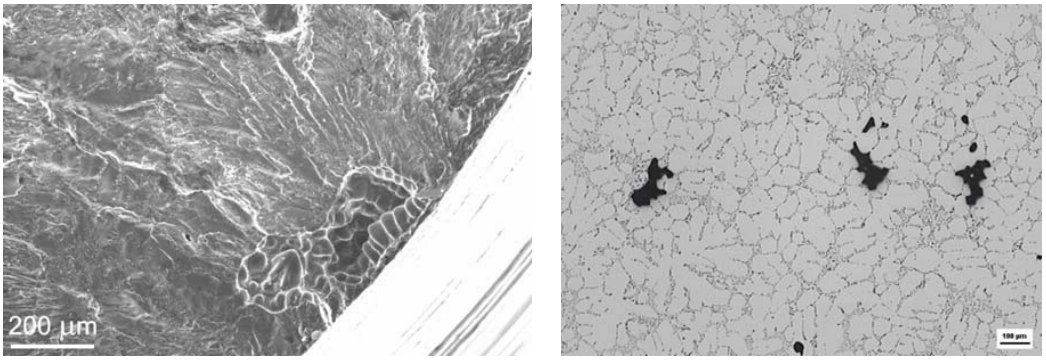

Fig. 1. a) Fracture surface showing fatigue initiation at a casting pore near the free surface; b) metallographic image of casting pores found in an Al-Si alloy

In this contribution two experimental techniques, namely X-ray computed tomography (XCT) and metallography, are applied on cast AlSi7Mg to separately characterize the size and morphology of casting pores. The 3D evidence provided by a modern tool, such as XCT, is used to discuss pore sizing criteria based on metallographic measurements. The role of pore morphology on fatigue is the discussed based on the stress concentration factor computed by the finite element analysis of a volume of material containing 3D pores obtained by XCT or 2D pores revealed by metallography.

2. Experimental methods

The material studied here is a cast AlSi7Mg that was previously tested in fatigue and found to be prone to crack initiation at pores, [11]. Fig. 1b shows the typical dendritic structure outlined by the dispersion of fine reinforcing particles of eutectic silicon. The spacing of the secondary dendritic arms (SDAS) is known to correlate with the local freezing rate, [12].

2.1. X-ray computed tomography

X-ray computed tomography (XCT) is a technology with increasing applications in material science, [13]. It exploits the penetrating power of a high density focused x-ray beam. The present experiments were performed at the Elettra Synchrotron facility in Trieste, Italy. The microtomographic-imaging set-up consists of a precision sample stage that allows for accurate rotation and translation of the sample and an electronic high-resolution detector system. Due to limitation of x-ray penetration the volume of material examined is limited (here a cylinder 4 mm in diameter and 1 mm in length). A schematic representation of the experiment is shown in Fig. 2. Initially, a large number of XCT scans of a material volume taken over 180° rotation are acquired (step 1 and 2 in Fig.2). These scans are projections of the specimen, representing pixel by pixel the absorption coefficient of the material crossed by X-rays. From these scans, cross-section images (i.e. slices) of the material volume were obtained with a back-

projection algorithm (Step 3 in Fig.2). Finally, the 3D reconstruction of pores from the series of slices is obtained via software (Step 4 in Fig.2).

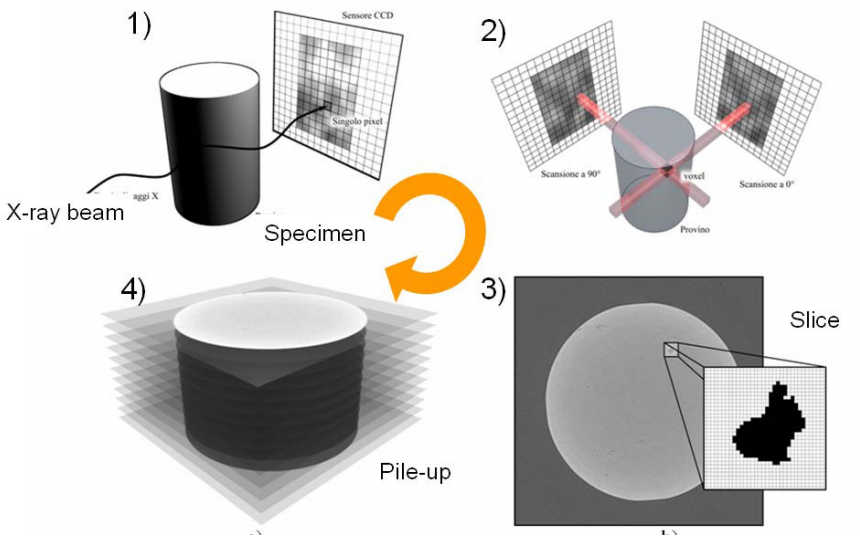

Fig. 2. Schematic of X-ray Computed Tomography XCT

The grey level images obtained after reconstruction were thresholded, in order to separate the pores from the rest of the material. The binary images were automatically analyzed giving the pore concentration and individual parameters such as volume, surface area, aspect ratios, etc.

2.2. Casting pore sizing and metallography

Metallography can be routinely used to study porosity in Al-Si castings and to compare casting processes. However, since it is unlikely that a random section through a pore will expose the maximum pore dimension. Therefore, direct metallographic measurements should not be input to fatigue life prediction models because it is the largest pore in a volume that will favour fatigue crack initiation. Previous studies demonstrated that pores observed on the fracture surfaces are 2 to 5 times larger than those observed on the metallographic planes regardless of the alloy and casting process, [9]. The Largest Extreme Value Distribution (LEVD) approach has been proposed to estimate the upper bound pore size of standard 2-D measurements of pore populations using metallographic observations, [10]. The approach is based on i) measurements of largest pore equivalent sizes found in a significant number of metallographic fields of view and iI) verification that data fit the Gumbel's distribution. In the affirmative case, the distribution is used for extrapolating pore sizes expected in large, realistic material cross-sections. A detailed description of the theoretical framework of the LEVD method is given elsewhere, [10].

An example of the LEVD approach is given in Fig. 3a where pore data sets obtained in the modified AlSi7Mg are entered into the Gumbel's plot. Since each data set appreciably fulfils the linearity condition, the fit statistical distributions can be used for extrapolation using the return period T parameter. Inspection of Fig. 2 shows that set A (modified with Na and cast in steel mold) has the largest pores followed by set B (modified with Sr and cast in steel mold) and set C (modified with Sr and sand cast). Since the slope of the regression line is an indicator of the data scatter, set B and C have similar and reduced scatter compared to set A.

However pore morphology poses a challenge to the metallographic characterization of largest pore sizes, namely when a definition of equivalent pore size is assumed to represent the actual 2D pore geometry. Pore morphology depends on the formation process and can be rounded in the case of gas pores or elongated in the case of shrinkage pores. The $(Area)^{1/2}$ parameter has been originally proposed for the LEVD method, [10]. More recently other definitions have been introduces, such as $4(Area)^{1/2}/\pi$ or Feret diameter, [8, 9], respectively. Fig.3b shows two casting pores in AlSi7Mg and two definitions of equivalent pore size, namely the maximum Feret diameter (i.e.

maximum distance between two points on the pore surface) and $(area)^{1/2}$ to represent the pore severity in fatigue. Quite different equivalent sizes are obtained. The Feret diameter is in both cases larger than the $(Area)^{1/2}$, but in the case of the rounded pore the difference is 50 % larger while in the case of elongated pore is more than 100 % larger.

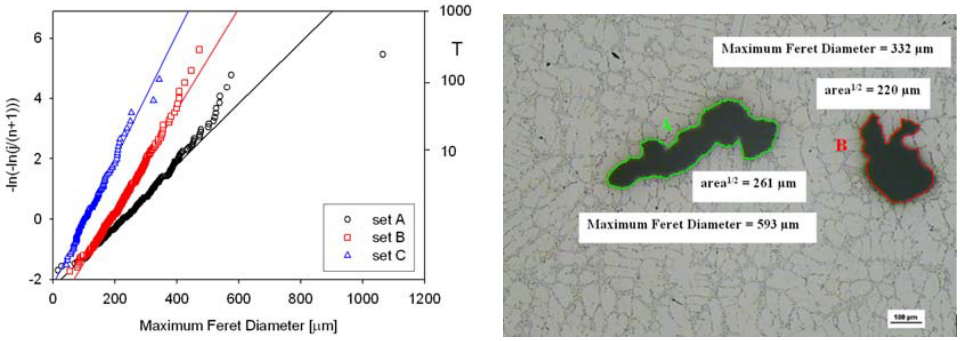

Fig. 3. (a) comparison of LEVD for three modifications of AlSi7Mg; (b) Alternative definitions of equivalent pore size

An additional issue that complicates the use of metallographic pore sizing for fatigue strength prediction is in the actual 3D morphology of cast pores because microshrinkage pores have a branched morphology because develop interdendritically and gas pores have a compact spherical shape due to the effect of the pressurized gas during freezing, [12].

3. Results and discussion

In this section the experimental 3D evidence of actual pore morphology obtained by XCT is initially presented and discussed. The implication on the metallographic measurement are then examined. Finally the stress concentration effect of the different morphologies are discussed with 3D finite element analysis.

3.1. 3D pore reconstruction by XCT

The XCT technique can visualize the distribution of pores within the small material volume as well as the morphology of each individual pore. Typically pore sizes found in industrial casting are in the 10 - 10^3 μm size range. Fig. 4 shows reconstructed two pores that are about 300 μm in maximum length.

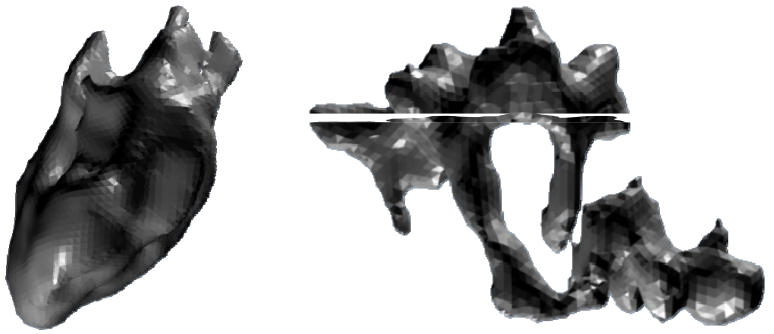

Fig. 4. Reconstructed XCT images of a) gas pore and b) shrinkage pore.

While it is not always straightforward to separate gas pores from shrinkage pores, Fig. 4a shows a reasonable representation of a gas pore and Fig. 4b of a shrinkage pore. The first pore is characterized by a Feret diameter:

312µm; volume: 0.00161mm^3; surface area: 0.09717 mm^2 and the second pore is characterized by a Feret diameter: 273µm; volume: 0.000372 mm^3; surface area: 0.0623 mm^2. The Feret diameter of the two pores is comparable while the volume of the shrinkage pore is one order of magnitude smaller than the gas pore.

While high-sensitivity XCT is still a quite sophisticated technology that can examine only small material volumes, the experimental evidence of Fig. 4 provides insight into different aspects of the application of metallography to pore size characterization in cast parts as will be discussed in the next subsections.

3.2. Metallographic sizing of casting pores

The metallographic evidence of casting pores shown of Fig. 1 and 3 is now reexamined in the light of the acquired understanding of the real pore morphology given by XCT. To model the sample preparation phase of metallography, the 3D pores of Fig. 4 are randomly sectioned to show the expected pore geometry in 2D. While only two examples are shown in Fig. 5 for obvious reasons, several consideration can be put forward based on these results. In the case of gas pores, a unique, connected region is generally found. The largest pore size is underestimated. The probability of finding isolated neighbouring pores belonging to the same pore such as Fig. 5a is very small.

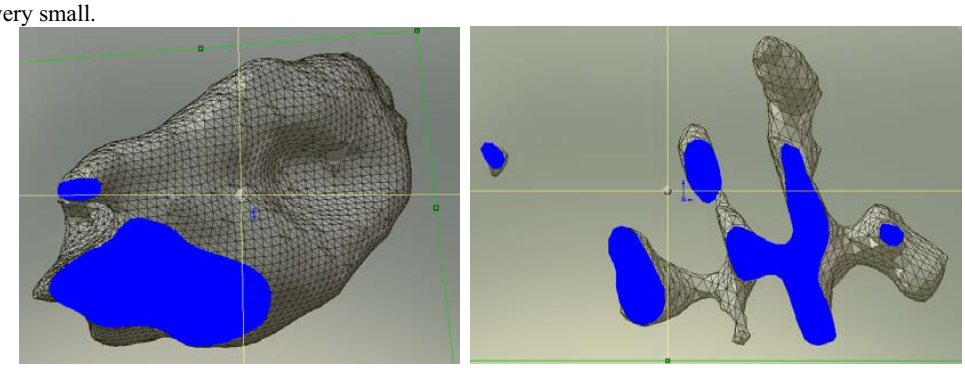

Fig. 5. Simulated sectioning of pores a) gas pore and b) shrinkage pore

In the case of shrinkage pores, the probability of finding neighboring pores belonging to the same pore, such as Fig. 5b, is the norm, (i.e. Fig. 1b). For its branched nature it is actually unlikely that the pore can appear as a unique connected region in a metallographic cross-section. Shrinkage pores will appear as multiple neighboring but isolated pores and the determination of the equivalent size of the largest of the multiple neighbouring pores results in a severe underestimate of the actual pore size.

Therefore, extrapolation required for estimating the expected largest pore in a material volume requires a return period T, [10], in the plot of Fig. 3a, which depend of the type of pore, i.e. gas or shrinkage. Alternatively, coalescence criteria should also be established to determine a realistic pore size as envelope of multiple isolated pores if they are expected to belong to the same shrinkage pore. The previous considerations demonstrate that pore morphology poses a challenge to the metallographic characterization of largest pore sizes for fatigue model development.

3.3. Comparison of estimated pore severity in fatigue

Pores in AlSi7Mg alloys are stress concentrators that favor localized damage leading to crack initiation and propagation in dependence of cyclic loading and residual stress. The severity of a pore in fatigue is known to increase with its equivalent size. However, the previous sections have demonstrated the role of equivalent pore size definition and of the type of pore on the largest pore size estimation to be used in fatigue life prediction. Now the influence the pore morphology on stress concentration is investigated by finite element FE modeling. The ABAQUS software (HKS Inc., Pawtucket, RI, USA) was used to determine the critical points and the local stress and strain concentration around casting pores.

The FE modeling activity used initially the metallographic evidence to generate plane strain 2D FE models containing pores that exactly matched the reality. Fig. 6a shows the micrograph of a shrinkage pore model and Fig. 6b the elastic stress distribution in the pore vicinity when loaded in the horizontal direction. The material model of the AlSi7Mg alloy was assumed to be elastic-linearly plastic, (i.e. modulus of elasticity: 69 GPa and Poisson's ratio: 0.33; tangent modulus: 1.3 GPa and yield stress: 200 MPa). The elastic stress concentration factor (K_t) defined as the ratio between the maximum Von Mises stress and the nominal stress is very high implying that local plasticity develops at low applied stress levels. The high K_t suggests that non propagating cracks may develop at notch roots of large pores. The result agrees with previous findings using the same approach, [8].

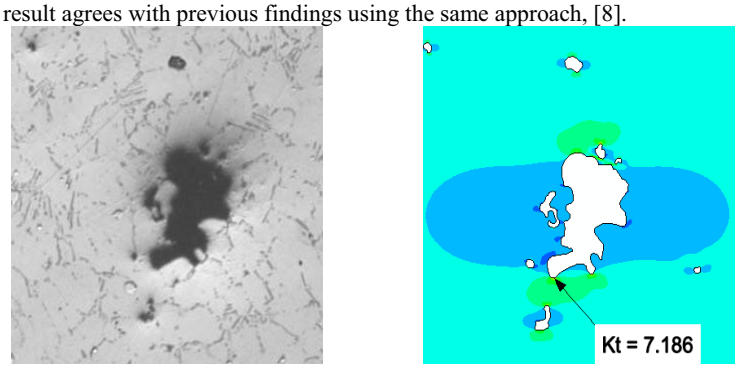

Fig. . 6: 2D stress distribution at a section through a shrinkage pore loaded in the horizontal direction

Subsequently, the reconstructed XCT pores of Fig. 4 were embedded in a FE model of a material volume to investigate the link between pore morphology in 3D and local stress concentration due to an applied load. Fig. 7 shows the procedure that was developed to exploit the XCT information. The pore geometry determined was smoothed and finely meshed and then embedded in a finite element model of a cylindrical volume (i.e. the central part of a push-pull fatigue specimen). Details of the fine tetraedral element mesh aimed at reproducing the pore surface is shown by a cross-section view through the pore. Fig. 7 shows also the local von Mises equivalent stress on the gas pore surface.

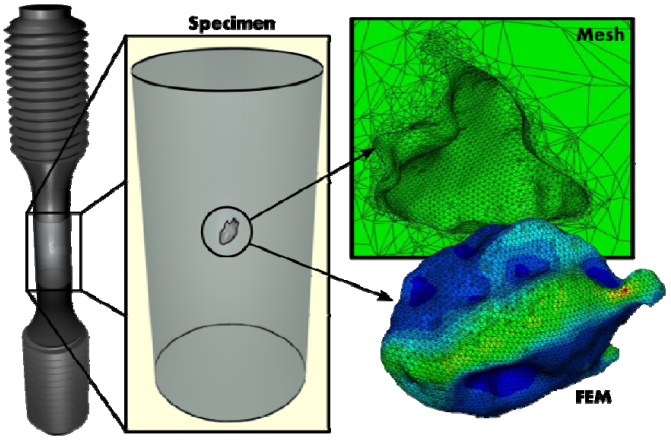

Fig. 7: Scheme of the finite element analysis of the stress concentration at the surface of a gas pore.

Due to its complex 3D geometry, the stress concentration factor K_t of a casting pore depends, not only on local notch root radius but also on the far-field load direction. Fig. 8 shows the results of the load direction with respect to the elastic stress concentration. The average K_t is about 3 and the max K_t for the most unfavorable load direction is about 3.5. Although not shown in detail here, gas and shrinkage pores have similar K_t because stress concentration

is mainly influenced by the local minimum radius of the pore surface, which is similar in the two cases. These K_t values in 3D are apparently lower than the results in 2D of Fig. 6. The motivation is in the 2D reduction of the actual 3D geometry. The K_t of a FE model obtained by sectioning the 3D pore in the manner shown in Fig. 5 reaches values similar to Fig. 6 (i.e. twice the 3D case). Previous studies adopted a simplified shape (i.e. spherical) in the modelling of the size effect and position with respect to the free surface instead of the real pore geometry, [8]. For an isolated spherical pore, $K_t \approx 2$, which is considerably lower than the present 3D result for a realistic pore. The current 3D FE modelling of realistic pores is expected to provide useful information for fatigue life prediction models of cast AlSi alloys.

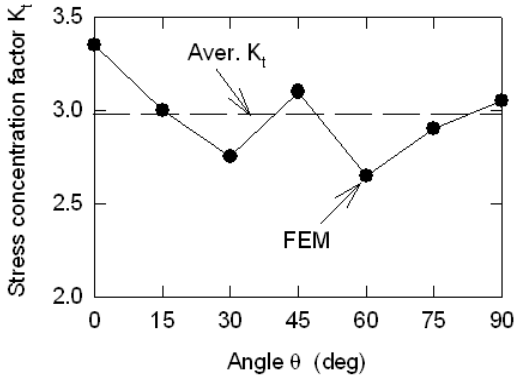

Fig. . 8: Stress concentration factor for a 3D gas pore loaded in different directions

4. Conclusions

Pores associated to the casting process are highly detrimental to the fatigue behavior of Al-Si alloys. The severity of casting pores in fatigue is related to a number of factors, such as pore size, morphology, position within the cast part, and so on. Here metallography was applied to the statistical pore size characterization of cast AlSi7Mg using the LEVD approach. However, the 2D nature of the metallographic information was expected to be a drawback when dealing with the complex 3D morphology, typical of shrinkage pores. X-ray computed tomography was therefore used to characterize the size and morphology of casting pores. The 3D evidence was then used to discuss equivalent pore sizing criteria based on metallographic measurements because shrinkage pores appear as multiple neighbouring pores with a severe underestimate of the actual pore size. The role of pore morphology on fatigue is also discussed based on the stress concentration factor computed by FE analysis of a volume of material containing 3D pores obtained by XCT and 2D pores revealed by metallography.

Acknowledgements

The corresponding author thanks Dr. Dreossi and Dr. Sodini at Elettra Sincrotrone Trieste for their contribution to image acquisition and analysis. Part of the work was supported under KEGA grant No.3/6110/08 and PRIN 2008.

References

[1] Wang QG, Apelian D, Lados DA. Fatigue behavior of A356-T6 aluminum cast alloys. Part I. Effect of casting defects. *J Light Metals* 2001;**1**:73–84.

[2] Couper, M. J., Neeson, A. E. and Griffiths, J. R. Casting defects and the fatigue behaviour of an aluminium casting alloy. *Fatigue Fract. Engng. Mater. Struct*. 1990;**13**:213–27.

[3] Sonsino, C. M. and Ziese, J. Fatigue strength and applications of cast aluminium alloys with different degrees of porosity. *Int. J. Fatigue* 1993;**15**:75–84.

[4] Skallerud B, Iveland T, Harkegard G. Fatigue life assessment of aluminum alloys with casting defects. *Eng Fract Mech* 1993;**44**:857–74.

[5] Dabayeh, A. A., Berube, A. J. and Topper, T. H. An experimental study of the effect of a flaw at a notch root on the fatigue life of cast Al 319. *Int. J. Fatigue* 1998;**20**,517–30.

[6] Buffiere J-Y, Savelli S, Jouneau PH, Maire E, Fougeres R. Experimental study of porosity and its relation to fatigue mechanisms of model Al–Si7–Mg0.3 cast Al alloys. *Mater Sci Eng A* 2001;**319**:115–26.

[7] Mayer H, Papakyriacou M, Zettl B, Stanzl-Tschegg SE. Influence of porosity on the fatigue limit of die cast magnesium and aluminum alloys. *Int J Fatigue* 2003;**25**:245–56.

[8] Gao YX, Yi JZ, Lee PD, Lindley TC. The effect of porosity on the fatigue life of cast aluminium-silicon alloys. *Fatigue Fract Eng Mater Struct* 2004;**27**:559.

[9] Wang Q. G., Jones P. E., Prediction of Fatigue Performance in Aluminium Shape Casting Containing Defects. *Metal. Matls Trans B* 2007;**38**:615-21.

[10] Murakami Y. *Metal Fatigue: Effects of Small Defects and Nonmetallic Inclusions*, Elsevier 2002.

[11] Nicoletto G., Baicchi P., Konečna R.,. Fatigue life prediction of AlSi alloys with casting defects, *Procs 2nd Fatigue Symp*, *Leoben*, 2008, 2-11.

[12] Anon. Properties and selection: nonferrous alloys and special-purpose materials. *ASM Handbook vol. 2* USA: ASM International, The Materials Information Society; 1990.

[13] Ferrie E, Buffiere JY, Ludwig W. 3D characterization of the nucleation of a short fatigue crack at a pore in a cast Al alloy using high resolution synchrotron microtomography. *Int J Fatigue* 2005;**27**:1215.

[14] Powazka P., et al., Computed tomography – an alternative and complement to traditional metallographic investigations of porosity in cast aluminum, *Procs 2nd Fatigue Symp*, *Leoben*, 2008, 51-66.